African Journal of Pharmaceutical Research and Development
Available online at https://ajopred.com
Vol. 16 No.3; pp. 12-24 (2024)

Original Research Article

DRUGGABILITY AND MOLECULAR DOCKING OF ESSENTIAL SECONDARY METABOLITES FROM *AZADIRACHTA INDICA* LEAF AGAINST ANGIOTENSIN CONVERTING ENZYME-2: COVID-19 IN FOCUS

PAUL CHIJIOKE OZIOKO[1*], UKAMAKA OWOHETETE[1], DANIEL DANLADI GAIYA[1]

1. Biology Unit, Faculty of Science, Air Force Institute of Technology (AFIT) Kaduna, Kaduna State, Nigeria.

ABSTRACT

Severe acute respiratory syndrome coronavirus 2 (SARS-CoV-2) is a highly infectious and virulent coronavirus that arose in late 2019 and poses great risk to public health and safety. The SARS-CoV-2 utilizes peptidase, angiotensin-converting enzyme 2 (ACE2) for entrance and invasion into host cells. Thus, this study explored the *in-silico* druggability and molecular docking of essential secondary metabolites (ESMs) from *Azadirachta indica* leaf as potential inhibitors of ACE-2, a main receptor for the SARS-CoV-2 virus causing the COVID-19 pandemic. Through a literature survey and database mining of known compounds from *A. indica* in the National Center for Biotechnology Information (NCBI) database, 12 secondary metabolites and 5 FDA COVID-19-approved drugs were identified. The *in-silico* druggability and molecular docking experiments were performed using SwissADME and ADMETlab tools, and Autodock vina and UCSF Chimera respectively. Discovery Studio was used for docking visualization and analyses of ligand-target interactions. The results suggest potential candidates for further consideration. Of the 12 secondary metabolites from *A. indica* and 5 FDA-approved drugs identified, azadirachtin A, azadirachtin D, azadirachtin H, azadirachtin F, azadirachtin I and nimbolin, and ivermectin showed relatively poor druggability. Of the 5 FDA-approved medications for the treatment of COVID-19 under investigation, only paritaprevir was able to dock (representing 20%); while 6 out of the 12 compounds from *A. indica* were able to dock perfectly (representing 50%). The best docking results identified paritaprevir, desacetylnimbin, azadiradione, nimbin, nimbolide, nimbinene, and azadirone as capable of binding to ACE-2 with the lowest free energy (binding score) of -14.60, -11.88, -11.60, -12.33, -12.78, -12.58, and -11.40 kcal/mol respectively. This study indicated that desacetylnimbin, azadiradione, nimbin, nimbolide, nimbinene, and azadirone from *A. indica* leaf are potent inhibitors of hACE2 with high druggability potentials. Hence, they are valuable natural bioactive compounds capable of targeting ACE-2 as potential therapeutics against the SARS-CoV-2 virus causing COVID-19.

ARTICLE INFO

Received 17 April, 2024
Accepted 05 December, 2024
Published 20 December, 2024

KEYWORDS
Azadirachta indica,
Druggability,
SARS-CoV-2,
Angiotensin converting enzyme-2,
Molecular docking,
ACE-2

INTRODUCTION

Coronavirus disease 2019 (COVID-19), also known as severe acute respiratory syndrome coronavirus 2 (SARS-CoV-2), is a highly infectious and virulent coronavirus that arose in 2019 [1]. It poses a risk to public health and safety. It is the third human coronavirus known to use the enzyme, angiotensin converting enzyme 2 (ACE2) to invade cells [2, 3]. Comprehending the cellular mechanism of SARS-CoV-2 action could lead to its management to prevent severe

***Corresponding author:** paulcj82@gmail.com; +234-703 531 0598

https://doi.org/10.59493/ajopred/2024.3.3 ISSN: 0794-800X (print); 1596-2431 (online)

disease and reduce death, which depends heavily on interaction between the SARS-CoV-2 and ACE2 [4]. Spike (S) protein is necessary for cell entry and membrane fusion, as it is for all coronaviruses [5-7]. The renin-angiotensin system is regulated by angiotensin converting enzyme 2 (ACE2), which reverses the negative effects of ACE on the cardiovascular system [3]. Angiotensin I is transformed by ACE into angiotensin II, a potent octapeptide with proinflammatory and vasopressor properties. The ACE is found in various animals, including pig, ferret, rhesus monkey, civet, cat, pangolin, rabbit, and dog. SARS-CoV-2 uses ACE2 receptors to replicate and infect alveolar epithelial cells in the lungs [2, 8]. The virus requires proteolytic processing of the S protein to activate the endocytic pathway through host of other proteases, such as TMPRSS2, cathepsin L, and furin [3, 5]

Currently to the best our knowledge, no antivirals or therapies have consistently proven successful against COVID-19 or SARS-CoV-2, while several medicines have shown some promise for specific patient subpopulations or end points. Therefore, drugs that can interfere with SARS-CoV-2's entrance processes may be a potential treatment. Researchers could focus on medicinal plants, as they are abundant in bioactive secondary metabolites. Hence, this study investigated the distinct bioactive chemicals from *Azadirachta indica* that have already been identified computationally. This plant was chosen because it is common and readily available in every season in Nigeria, and used locally in the management of malaria, typhoid, high sugar level, and other ailments.

Azadirachta indica Linn, referred to as neem, is a tropical evergreen tree native to India and Southeast Asia [9]. It blongs to the *Meliaceae*, or mahogany family. According to Hossain and Nagooru [10] and Ghimeray *et al*. [11], it is known as the "Life Giving Tree," "Nature's Drugstore," "Village Pharmacy," and "Panacea for All Diseases" in India. It is well documented for its medicinal efficacies, including antiviral, anti-inflammatory, anti-ulcer, anti-fungal, antibacterial, antiseptic, antipyretic, and anti-diabetic properties [12-14]. The leaves of neem contain numerous bioactive compounds, including azadirachtin-A, that was found to inactivate the SARS-CoV-2 virus protease [15-18]. As human ACE2 is essential for COVID-19 entrance and invasion into host cells, this research was aimed to explore the *in-silico* druggability and virtual screening of bioactive chemicals from *A. indica* leaf that may have potential inhibitory effects on human ACE2, a key component of COVID-19.

MATERIALS AND METHODS

Ligands

In the works of Loganathan *et al*. and Mohammad and Forough, some unique secondary metabolites (ligands) (that are not common in other plants) were identified from the leaf of *A. indica* [19, 20]. Their two-dimensional (2-D) structures were obtained from the PubChem database of the National Center for Biotechnology Information (NCBI) (https://pubchem.ncbi.nlm.nih.gov) [21]. The compounds chosen from *A. indica* leaf were: azadirachtin-A, azadirachtin-D, azadirachtin-H, azadirachtin-F, azadirachtin-I, desacetylnimbin, azadiradione, nimbin, nimbolin, nimbolide, nimbinene, and azadirone. Similarly, some FDA-approved drugs for the treatment of COVID-19, such as remdesivir, baricitinib, paritaprevir, ivermectin, and 2-monolinolenin, were equally retrieved from PubChem.

In-Silico Druggability Prediction

The physicochemical properties of the ligands were predicted using the SwissADME tool (http://www.swissadme.ch) and the ADMETlab tool [22]. The prediction of druggability or drug-likeness of these compounds was equally carried out using the SwissADME online tool [23] according to Lipinski's rule of 5 (LR5). This web server evaluates the compound's drug likeness using Lipinski's Rule [24], which confirms the property of an oral drug for the compounds.

Human Angiotensin Converting Enzyme-2 (hACE-2) Target

The SARS-CoV-2 RBD-hACE2 (code: 6VW1) proteins were downloaded and obtained from the protein data bank (PDB) (http://www.rcsb.org/pdb/) [24].

Molecular Docking Using AutoDock Vina

AutoDock Vina 1.2.0 docking software program [25] and UCSF Chimera [26] were used for docking studies to examine the structural connection between receptor and ligand. Blind docking process was used in which the Grid Box was chosen to cover the whole probable binding pocket of the target, ACE2.

Preparation of Ligands and Targets

The ACE2 target by adding hydrogen atoms, eliminating non-crystallographic water molecules, adding partial charges, and indicating protonation status of the residues of amino acid [27]. Besides, other ligands and non-standard residues attached to the main target chain were deleted.

The ligands (both from *A. indica* leaf and FDA-approved COVID-19 drugs) were also prepared for docking, which involves adding hydrogen atoms, desolvation of water molecules, adding partial charges, and structural minimization.

Visualization and Analysis of Docking Interactions
Using Discovery Studio v21.10.20298, the target-ligand docked complex was visualized and interactions analyzed [28]. This molecular visualization tool was used to examine the intermolecular bonding interactions between the protein and the ligands as well as predict the distance of hydrogen bond formation between them.
Note: The inhibition constant, Ki, was calculated from the binding score (or binding energy or affinity) obtained from best docking pose after ranking, using equation 1.

Ki= $e^{\Delta G/RT}$ .....Equation 1

Where ΔG = free energy change (or binding energy) in Kcal/mol, R= universal rate constant ($1.987x10^{-3}$Kcal.mol^{-1}. K^{-1}), and T= absolute temperature (298K).

RESULT

***In-silico* physicochemical properties**
Table 1 shows the molecular formula and PubChem CID of the ligands investigated.

Figures 1a and 1b are the 2-D molecular structures of the ligands drawn with ChemDraw Pro 8.0.

The qualitative evaluation of the solubility class is assigned using the following log *S* scale: insoluble 10 <poorly 6 <moderately 4 <soluble 2 <very <0 <highly. All the predicted values in SwissADME are the decimal logarithm of the solubility in water (log *S*) (Table 2).

Prediction of druggability properties
The prediction of druggability or drug-likeness properties of the molecules was in line with Lipinski's rule of 5 (LR5). Here, the ligands' lipophilicity, number of hydrogen bond acceptors and donors, molecular weight, oral bioavailability score, and the number of Lipinski's rule violations were predicted (Table 3).

Prediction of pharmacokinetic profiles of ligands
The pharmacokinetic profiles predicted were the absorption and distribution (Table 4), and excretion as well as the toxicological parameters (Table 5).

Table 6 presented the basic properties of ligand-target complex interactions as visualized with Discovery Studios. However, the Ki was calculated from binding energy obtained from the best ligand pose after ranking.

Molecular docking of the ligands with the target protein (ACE2)
Following the druggability and physicochemical properties predictions of the compounds under investigation, remdesivir, ivermectin, azadirachtin A, azadirachtin D, azadirachtin H, azadirachtin F, azadirachtin I, and nimbolin showed poor physicochemical and druggability properties. Despite this, all the ligands were subjected to molecular docking (MD) to elucidate their interactions with ACE-2, which is essential in the invasion of SARS-CoV-2 into its host organisms. Docking all the ligands will allow us to correlate their physicochemical properties and drug-likeness potential with that of docking interactions with the target.
The ACE2, in which the S protein of SARS-CoV2 has sufficient affinity for human cells, was retrieved from PDB (6VW1) for SARS-CoV-2 RBD-hACE2 (Figure 2).

Note that in Table 5, 1 and 0 are categorical, which mean **positive** and **negative,** respectively, with different probabilities (although not shown here). For instance, hERG 0 means non-blocker, while 1 means blocker.

Figure 3 represents the prepared structure of ACE2 (by adding hydrogen atoms, eliminating non-crystallographic water molecules, adding partial charges, and indicating the protonation status of the residues of amino acid) used for the docking study.

Of the 5 FDA-approved drugs and the 12 selected compounds from *A. indica* used for the docking studies, 1 (20%) and 6 (50%), respectively, were successfully docked. Thus, if these compounds were purely isolated from *A. indica* leaves, they could be harnessed for the management and treatment of COVID-19

.

Table 1: Ligands and Their PubChem CID

S/N	Ligands	PubChem CID	Molecular Formula
1.	Remdesivir	121304016	$C_{27}H_{39}N_6O_8P$
2.	Baricitinib	44205240	$C_{16}H_{21}N_7O_2S$
3.	Paritaprevir	45110509	$C_{40}H_{43}N_7O_7S$
4.	Ivermectin	6321424	$C_{48}H_{74}O_{14}$
5.	2-monolinolenin	11674746	$C_{21}H_{36}O_4$
6.	Azadirachtin A	4369359	$C_{35}H_{44}O_{16}$
7.	Azadirachtin D	65981	$C_{34}H_{44}O_{144}$
8.	Azadirachtin H	16134956	$C_{33}H_{42}O_{14}$
9.	Azadirachtin F	131750885	$C_{33}H_{44}O_{14}$
10.	Azadirachtin I	5281303	$C_{33}H_{44}O_{14}$
11.	Desacetylnimbin	5281654	$C_{28}H_{34}O_8$
12.	Azadiradione	5316860	$C_{28}H_{34}O_5$
13.	Nimbin	108058	$C_{30}H_{36}O_9$
14.	Nimbolin	6443005	$C_{39}H_{46}O_{10}$
15.	Nimbolide	12313376	$C_{27}H_{30}O_7$
16.	Nimbinene	44715635	$C_{28}H_{34}O_7$
17.	Azadirone	10906239	$C_{28}H_{36}O_4$

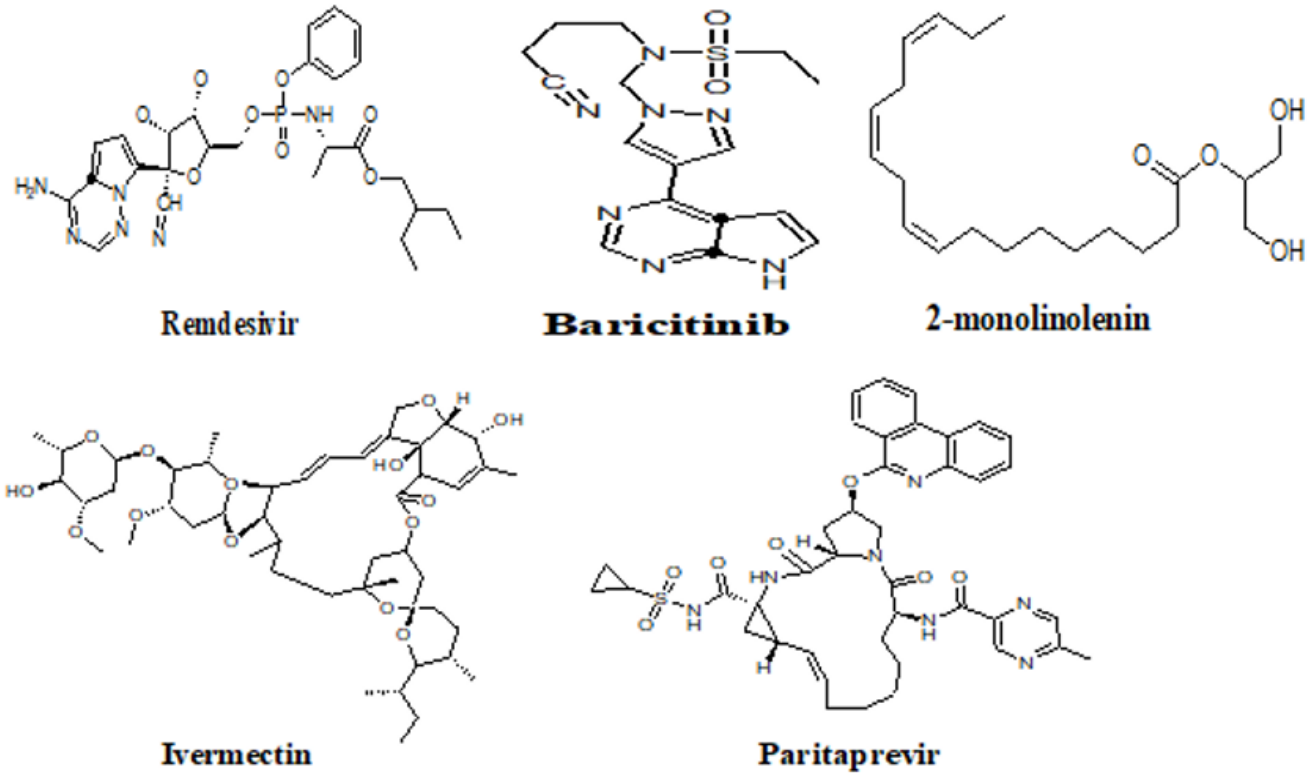

Figure 1a: The 2-D Chemical structures of the FDA-approved drugs for the management of COVID-19

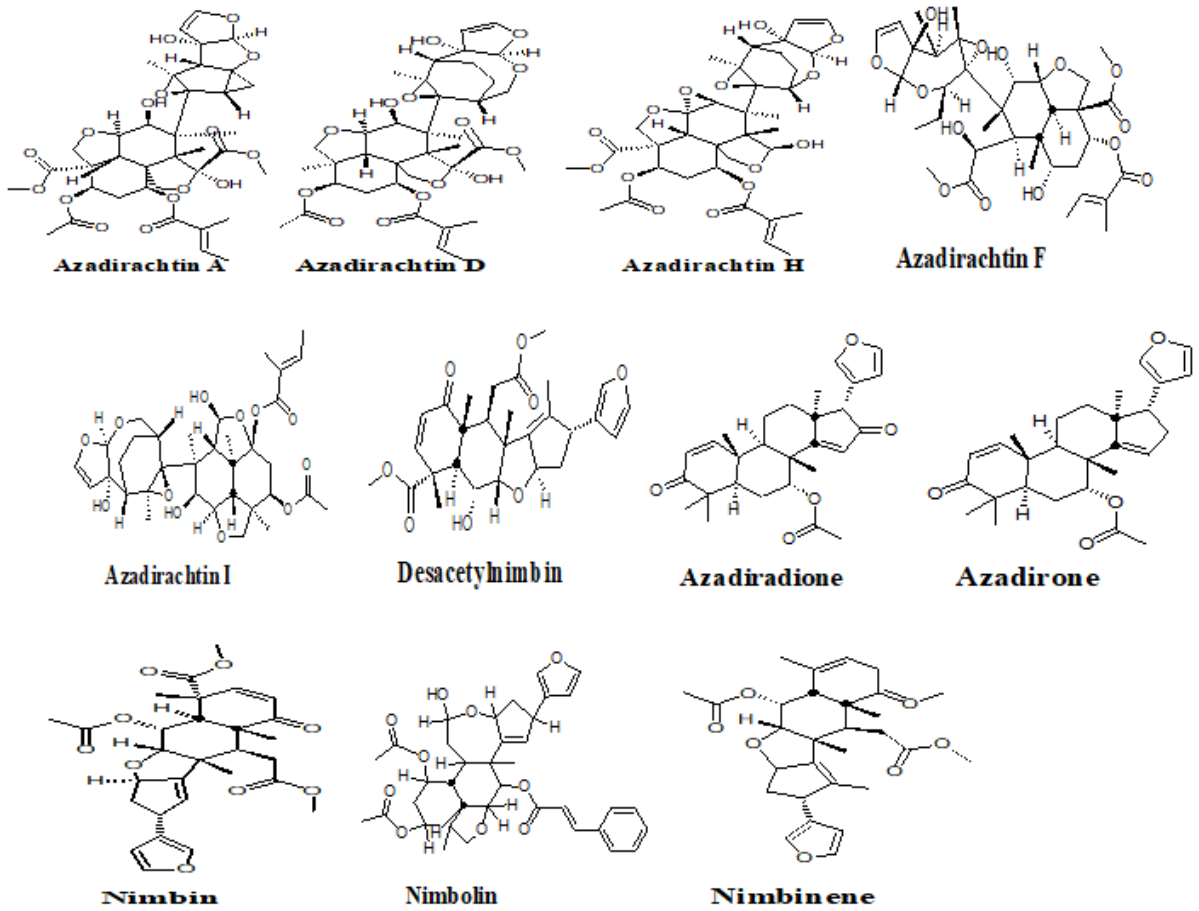

Figure 1b: The 2-D Chemical structures of the FDA unique compounds from *A. indica* leaf

Table 2: The Physicochemical Properties of the Ligands

Ligands	Properties							
	No HA	No Aro HA	F Csp3	No RB	MR	TPSA	ESOL Solubility Solubility (mg/ml)	Class
Remdesivir[2]	42.00	15.00	0.52	15.00	153.39	215.59	0.184	Soluble
Baricitinib[1]	26.00	14.00	0.44	6.00	101.47	131.17	7.31	Very Soluble
Paritaprevir[4]	55.00	20.00	0.42	9.00	211.96	198.03	$0.49x10^{-4}$	Poorly Soluble
Ivermectin[4]	62.00	0.00	0.81	8.00	230.77	170.06	$0.16x10^{-5}$	Poorly Soluble
2-monolinolenin[2]	25.00	0.00	0.67	17.00	105.25	66.76	$3.16x10^{-2}$	Moderately Soluble
Azadirachtin A[2]	51.00	0.00	0.77	10.00	165.92	215.34	$3.33x10^{-2}$	Moderately Soluble
Azadirachtin D[2]	48.00	0.00	0.79	8.00	159.83	189.04	$1.06x10^{-2}$	Moderately Soluble
Azadirachtin H[2]	47.00	0.00	0.79	8.00	154.98	189.04	$3.40x10^{-2}$	Moderately Soluble
Azadirachtin F[2]	47.00	0.00	0.79	9.00	157.18	200.04	$3.19x10^{-2}$	Moderately Soluble
Azadirachtin I[2]	44.00	0.00	0.81	6.00	148.89	162.74	$1.07x10^{-2}$	Moderately Soluble
Desacetylnimbin[2]	36.00	5.00	0.61	6.00	129.07	112.27	$9.61x10^{-2}$	Moderately Soluble
Azadiradione[4]	33.00	5.00	0.61	3.00	125.48	73.58	$1.17x10^{-3}$	Moderately Soluble
Nimbin[3]	39.00	5.00	0.60	8.00	138.81	118.34	$3.45x10^{-2}$	Moderately Soluble
Nimbolin[4]	49.00	11.00	0.56	9.00	178.44	130.73	$1.82x10^{-4}$	Poorly Soluble
Nimbolide[3]	34.00	5.00	0.59	4.00	120.00	92.04	$5.30x10^{-2}$	Moderately Soluble
Nimbinene[3]	35.00	5.00	0.61	6.00	128.17	92.04	$7.19x10^{-2}$	Moderately Soluble
Azadirone[4]	32.00	5.00	0.64	3.00	125.28	56.51	$3.73x10^{-4}$	Poorly Soluble

Key: No HA = Number of heavy atoms; No Ar HA = Number of aromatic heavy atoms; F Csp3 = Fraction of carbon sp3; No RB = Number of rotatable bonds; MR = Molecular refractivity; TPSA = Topological polar surface area; ESOL= Estimated Solubility. The ligands with superscripts 1, 2, 3, and 4 are said to be very soluble, soluble, moderately soluble, and poorly soluble, respectively.

Table 3: Predicted drug-likeness of the ligands

Ligands	Parameters					
	C Log $P_{o/w}$	No HBA	No HBD	MW(g/mol)	Lip V	B Score
Remdesivir	1.24	12.00	5.00	606.61	2.00	0.17
Baricitinib	0.41	7.00	2.00	375.45	0.00	0.55
Paritaprevir	2.75	10.00	3.00	765.88	2.00	0.17
Ivermectin	4.37	14.00	3.00	875.09	2.00	0.17
2-monolinolenin	4.66	4.00	2.00	352.51	0.00	0.55
Azadirachtin A	1.08	16.00	3.00	720.71	2.00	0.17
Azadirachtin D	1.55	14.00	3.00	676.70	2.00	0.17
Azadirachtin H	1.13	14.00	3.00	662.68	2.00	0.17
Azadirachtin F	0.98	14.00	4.00	664.69	2.00	0.17
Azadirachtin I	1.81	12.00	3.00	618.67	2.00	0.17
Desacetylnimbin	2.76	8.00	1.00	498.56	0.00	0.55
Azadiradione	4.34	5.00	0.00	450.57	0.00	0.55
Nimbin	3.24	9.00	0.00	540.60	1.00	0.55
Nimbolin	4.46	10.00	1.00	674.78	1.00	0.55
Nimbolide	3.11	7.00	0.00	466.52	0.00	0.55
Nimbinene	3.44	7.00	0.00	482.57	0.00	0.55
Azadirone	5.06	4.00	0.00	436.58	1.00	0.55

Key: C = consensus; MW = Molecular weight; No HBA = Number of hydrogen bond acceptors; No of HBD = Number of hydrogen bond donors; Lip V = Lipinski Violation; B = Bioavailability.

Table 4: Absorption and distribution of the ligands

Ligands	Parameters			
	GIA	BBB	P-gp S	Log K_p(cm/s)
Remdesivir	Low	No	Yes	-9.28
Baricitinib	High	No	Yes	-9.11
Paritaprevir	Low	No	Yes	-7.67
Ivermectin	Low	No	Yes	-7.14
2-monolinolenin	High	Yes	No	-4.91
Azadirachtin A	Low	No	Yes	-9.92
Azadirachtin D	Low	No	Yes	-8.97
Azadirachtin H	Low	No	Yes	-9.36
Azadirachtin F	Low	No	Yes	-9.28
Azadirachtin I	Low	No	Yes	-8.41
Desacetylnimbin	High	No	No	-8.13
Azadiradione	High	No	Yes	-5.63
Nimbin	High	No	No	-7.98
Nimbolin	Low	No	Yes	-7.06
Nimbolide	High	No	Yes	-7.61
Nimbinene	High	No	No	-7.80
Azadirone	High	No	No	-4.90

Key: GIA = gastrointestinal absorption; BBB P = blood brain barrier permeant; P-gp = P-glycoprotein; S=substrate; Log K_p = skin permeation. 'Yes' and 'No' respectively connote a higher tendency of the ligand being a substrate or non-substrate of P-gp and permeating the BBB or not.

Table 5: Excretion and toxicity of the ligand

Ligands	Parameters							
	Excretion		Toxicity					
	$T^1/_2$(hr)	CL (mL/min/kg)	hERG Blocker	H-HT	AMES	Skin Sen.	LD_{50} (log[1/mol/kg])	DILI
Remdesivir	1.39	0.74	1.00	1.00	0.00	0.00	2.99	1.00
Baricitinib	1.47	1.16	0.00	1.00	0.00	0.00	2.52	1.00
Paritaprevir	2.19	0.82	1.00	0.00	0.00	0.00	3.10	1.00
Ivermectin	2.43	1.04	1.00	0.00	0.00	0.00	3.68	0.00
2-monolinolenin	1.80	1.60	1.00	0.00	0.00	1.00	1.46	0.00
Azadirachtin A	2.05	1.37	0.00	0.00	0.00	0.00	3.74	0.00
Azadirachtin D	1.94	1.38	0.00	0.00	0.00	0.00	3.73	0.00
Azadirachtin H	1.92	1.49	0.00	0.00	0.00	0.00	3.86	0.00
Azadirachtin F	1.99	1.53	0.00	0.00	0.00	0.00	3.94	0.00
Azadirachtin I	1.75	1.46	0.00	0.00	0.00	0.00	3.98	0.00
Desacetylnimbin	1.45	1.77	0.00	0.00	0.00	0.00	3.76	0.00
Azadiradione	1.73	1.88	0.00	1.00	0.00	0.00	3.59	0.00
Nimbin	1.69	1.65	0.00	1.00	0.00	0.00	3.76	1.00
Nimbolin	2.15	1.60	1.00	1.00	0.00	0.00	4.25	1.00
Nimbolide	1.41	1.92	0.00	0.00	0.00	0.00	3.94	1.00
Nimbinene	1.41	1.77	0.00	1.00	0.00	0.00	3.70	0.00
Azadirone	1.87	1.70	1.00	1.00	0.00	0.00	3.42	0.00

Key: $T^1/_2$ = Half-time; CL= clearance; Herg = human ether-a-go-go-related gene; H-HT = human hepatotoxicity; AMES = Ames mutagenicity; SkinSen = skin sensitivity; LD_{50} = median lethal dose; DILI = drug induced liver injury.

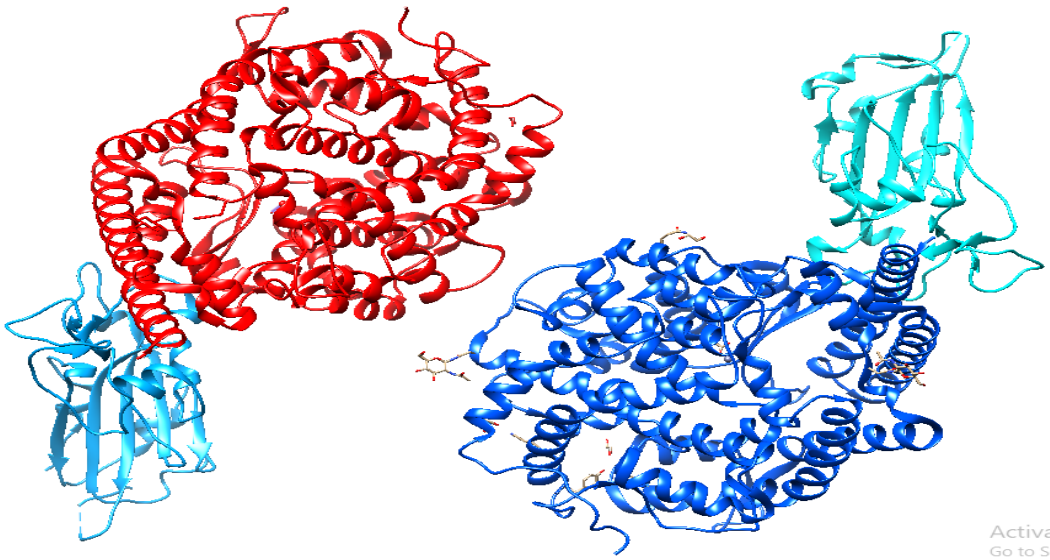

Figure 2: 3D Structure of SARS-CoV-2 chimeric receptor-binding domain (RBD) complexed with its receptor human ACE2 (ACE2 chains are coloured red and blue in domain A and B respectively)

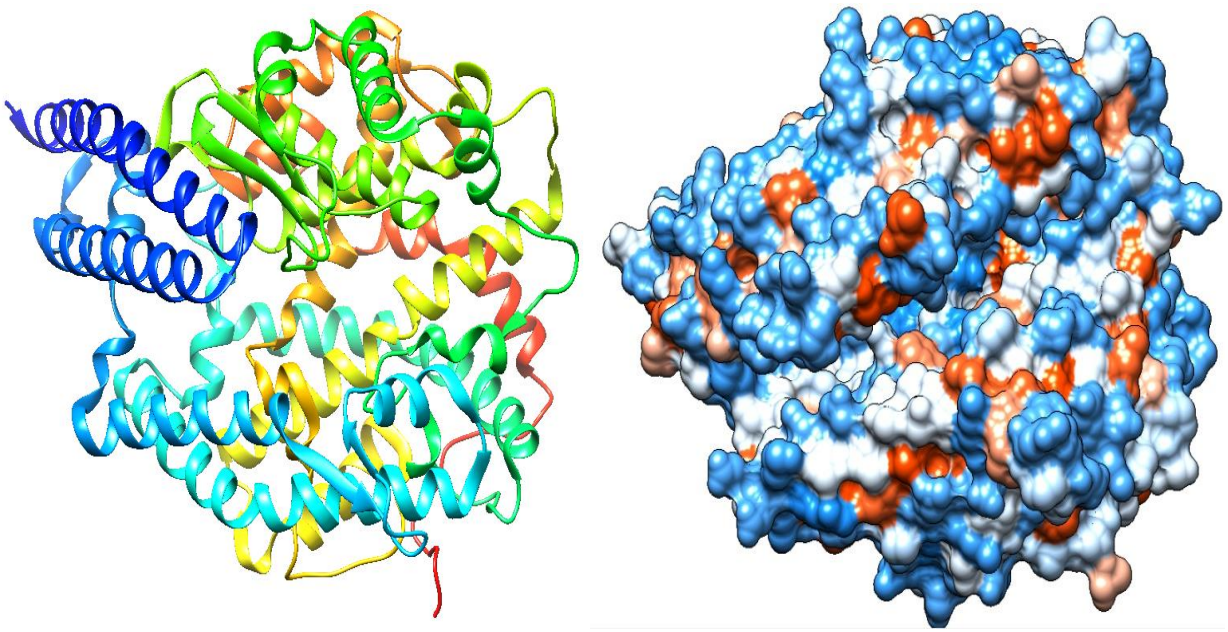

A B

Figure 3: 3-D Ribbon structure (A) and hydrophobicity surface (B) of prepared ACE2.

Table 6: Basic properties of the ligand-protein complexes from docking interaction

Ligands	Parameters			
	BE Kcal/mol)	NHBs	Ki(nM)	Amino acids involved in interaction
Paritaprevir	-14.62	4.00	$1.93x10^{-2}$	Trp349, Asp350, Glu375, Asp382, His401, Glu402, and Zn704.
Desacetylnimbin	-11.88	3.00	$18.94x10^{-1}$	Leu370, Thr371, **His374**, Glu375, Glu402, **Glu406**, Ser409, Thr445, Ile446, Tyr515, and Arg518.
Azadiradione	-11.63	4.00	$29.19x10^{-1}$	Arg273, Phe274, Leu370, Thr374, **His374**, **Glu406**, Ser409, Ala413, Thr445, Ile446, Tyr515, and Arg518.
Nimbin	-12.33	5.00	$8.95x10^{-1}$	Arg273, **His374**, Glu375, Glu402, **Glu406**, and Gln442.
Nimbolide	-12.78	3.00	$4.18x10^{-1}$	Phe40, Ser44, Ser47, Asn51, Thr347, Ala348, Trp349, Asp350, and Leu351.
Nimbinene	-12.58	3.00	$5.86x10^{-1}$	Phe40, Ser44, Ser47, Asn51, Thr347, Ala348, Trp349, Asp350, and Leu351.
Azadirone	-11.40	4.00	4.30	Thr371, Asp367, **His374**, Leu370, **Glu406**, and Ser409.

Key: BE = binding energy; NHBs= number of hydrogen bonds; Ki= Inhibition Constant; H= hydrogen; A.A.= amino acid

DISCUSSION

This research investigated *in-silico* druggability and virtual screening of bioactive chemicals from *A. indica* leaves that may have potential inhibitory effects on human ACE2, essential for COVID-19 entrance and invasion into host cells. According to the findings of the physicochemical characteristics' predictions (Table 2), the fraction of carbon Sp3 is predicted to be between 0.25-1, and the maximum number of RBs for determining the unsaturation and flexibility of the chosen ligands or compounds should not be more than 9. Similar to this, molecules that have a TPSA higher than 140 $Å^2$ tend to be poor at penetrating cell membranes. As observed in the instance of the 2-monolinolenin molecule (Table 2).

According to [29], molecules having a TPSA of more than 140$Å^2$ often have limited membrane penetration, and these molecules have been classified as poorly absorbed. Also, oral drug candidates with more than three aromatic rings are less likely to be developed successfully than those with fewer. Thus, from our findings, the majority of ligands are fairly soluble, except nimbolin and azadirone, which are weakly soluble. Baricitinib, an electrophilic ligand with a benzene ring and nitrogen atoms, is extremely soluble. Low solubility of other ligands could result from lack of hydroxyl groups on ligands structures (Figure 1) and thus little or no inter-hydrogen bond formations and no electron donating ability.

Additionally, the results of lipophilicity (Table 3) revealed that all ligands, with the exception of azadirone, have logP values less than 5. According to LR5 suggestions [24], which forecast a novel synthetic molecule's drug-likeness, include Log*P* as a key property, and all of the compounds investigated fell within the limit set. An optimal range for lipophilicity for a compound's oral and intestinal absorption is 1.35–1.8. The digits 0, 1, and 2 under the Lipinski rule violation column, respectively, denote no (zero), one, and two violations of the rule (Table 3). Any ligand or molecule that does not have more than one infraction of LR5 is deemed to have good drug-likeness or druggability and may also have lead-likeness. In order to increase the prediction potential by consensus log $P_{o/w}$, models underlying the predictors for lipophilicity should be as diverse as possible [30]. Thus, SwissADME provided opportunity to five publicly available predictive models: XLOGP3 [31], WLOGP [32], MLOG [33], SILICOS-IT, a hybrid method depending on 27 fragments and 7 topological descriptors, and finally iLOGP, a physics-based model using free energies of solvation. The average values of these models gave the ClogP value. The Abbot Bioavailability Score [34] (Table 3) predicts the likelihood of a chemical having measurable Caco-2 permeability or at least 10% oral bioavailability in rats. This semi-quantitative rule-based score establishes 4 classifications of ligands with probabilities of 11%, 17%, 56%, or 85%, and is dependent on total charge, TPSA, and infraction of the Lipinski filter. So, the bioactivity scores for baricitinib, 2-monolinolenin, desacetylnimbin, azadiradione, nimbin, nimbolin, nimbolide, nimbinene, and azadirone are in agreement with their drug-likeness.

The formulation of oral medication candidates is heavily influenced by the absorption and distribution of medicines or ligands predicted by ADMET properties (Table 4). The Kp is linearly correlated with molecule size and LogP [35], and less skin-permeable the molecule, the more negative the log Kp. According to this finding, skin sensitivity was greatest for the values in blue and least for those in red (Table 4). Additionally, understanding which substances are substrates or non-substrates of the P-gp is essential to evaluate active efflux through cellular membranes. The central nervous system's defense against xenobiotics is one of P-gp's key functions [36]. As indicated in the result, 2-monolinolenin can only penetrate the BBB, suggesting its potential as a CNS drug.

The majority of substances, except remdesivir and nimbolin, demonstrated minimal toxicity and low oral acute toxicity, with the exception of 2-monolinolenin. All drugs had an excretion half-life of 1 to 3 hours and a clearance time of 2 mL/min/kg. However, ivermectin, azadirachtin A, azadirachtin D, azadirachtin H, azadirachtin F, azadirachtin I, and nimbolin demonstrated very low physicochemical properties and drug-likeness projections (Table 5). The majority of the substances, with the exception of remdesivir and nimboline, have a relatively low level of toxicity. However, for 2-monolinolenin, its oral acute toxicity can also be claimed to be quite low [37]. In analyzing docking interactions, the docking poses or conformations with the least BE score were selected after docking, and visualized using DS Studio. Remdesivir, baricitinib, 2-monolinolenin, ivermectin, azadirachtin A, azadirachtin D, azadirachtin H, azadirachtin F, azadirachtin I, and nimbolin were the ligands that could not dock at the enzyme's binding site. This inability of these compounds to dock at the active site of ACE2 could result from structural steric hindrances. These aforementioned ligands did not also show good druggability and physicochemical properties (Tables 2 and 3). Of the 5 FDA-approved oral medications for treatment of COVID-19 under investigation, only paritaprevir was able to dock (representing 20%), while 6 out of the 12 compounds from *A. indica* were able to dock perfectly (representing 50%).

The binding energy and free energy (ΔG) were used to calculate the variation during the development of the ligand-receptor complex. The main purpose of structure-based drug design (SBDD) has reportedly been stated to be an *in-silico* prediction of the ΔG of ligand-protein binding [38]. According to the data (Table 6), paritaprevir had the highest negative BE of all the ligands, that might be related to the metal Zn704, which may have helped with the binding affinity and stability of the enzyme-ligand complex. Almost 80% of the complexes' binding interactions involved the residues His374 and GLU406. Therefore, these amino acids may play a crucial role in regulating ACE2 catalytic action. The binding affinities or inhibition constants of nimbin, nimbolide, and nimbinene are roughly equivalent. This could result from structural similarities between them. Desacetylnimbin, azadiradione, and azadirone similarly have close binding affinity which may equally be due to their structural resemblance. Similar to this, the quantity of hydrogen bonds, as well as other bonding interactions, is crucial for maintaining the stability between the target and ligand complex.

These *A. indica* leaf compounds (desacetylnimbin, azadiradione, Nimbin, nimbolide, nimbinene, and azadirone) have good druggability and physicochemical properties as well as Ki in nM scale, suggesting that they may be the "save" bioactive compounds that the world is looking for as a long-term treatment for COVID-19 and possibly other deadly viruses that may emerge in the future. Furthermore, as *A. indica* is a good source of these substances [19, 20], herbal preparation, in form of supplement, of this plant's leaf extract for local SARS-CoV-2 treatment and management may show promise.

CONCLUSION

This study revealed that the physicochemical properties and drug-likeness predictions of ivermectin, azadirachtin A, azadirachtin D, azadirachtin H, azadirachtin F, azadirachtin I, and Nimbolin were somewhat subpar compared to the other ligands studied. Most of the substances (such as azadirachtin A, azadirachtin D, azadirachtin H, azadirachtin F, azadirachtin I, desacetylnimbin, azadiradione, nimbin, nimbolide, nimbinene, and azadirone), with the exception of remdesivir and nimboline, have a relatively low level of toxicity. Additionally, the docking of remdesivir, baricitinib, 2-

monolinolenin, ivermectin, azadirachtin A, azadirachtin D, azadirachtin H, azadirachtin F, and azadirachtin I at the ACE2 enzyme's binding site was unsuccessful. Comparatively, 50% of the compounds from *A. indica* docked well, as opposed to 20% of the ligands from FDA COVID-19-authorized medications under research. This study indicated that desacetylnimbin, azadiradione, nimbin, nimbolide, nimbinene, and azadirone, which are all derived from *A. indica* leaves are potent inhibitors of hACE2 with high druggability potentials. Hence, they are valuable natural bioactive compounds capable of targeting ACE-2 as a potential therapeutics against the SARS-CoV-2 virus causing COVID-19. Also, leaf extract of this plant, which is a good source of these chemicals, may be used in herbal supplement formulations to treat or manage SARS-CoV-2 locally.

RECOMMENDATION

We recommend that these bioactive molecules from *A. indica* leave be isolated and their respective inhibitory potentials on human ACE2 be determined in *in-vitro* and *in-vivo* experiments. Also, various leaf extracts of the plant can be formulated and applied in treatment of SARS-Cov-2 locally in ethno-medicinal practices.

ACKNOWLEDGEMENT

Not applicable.

AUTHORS' CONTRIBUTION

P.C. Ozioko conceptualized and designed the work. He puts the manuscript pen to paper. U. Owohetete co-designed the work and edited the manuscript, while D.D. Gaiya suggested the software used for work and equally edited the manuscript.

CONFLICT OF INTEREST

The authors declare that there is no conflict of interest, be it funding or otherwise. All authors read and approved the revised manuscript.

FUNDING

No funding was provided. It was self-sponsored by the authors.

ABBREVIATIONS

ABCs	ATP-binding cassette transporters
ACE2	Angiotensin converting enzyme 2
ADMET	Absorption, distribution, metabolism, excretion, and toxicity
AMES	Ames mutagenicity
BBB	Blood-brain barrier
BE	Binding energy
CADD	Computer-aided drug design
CL	Clearance
COVID-19	coronavirus disease 2019
CYP	Cytochrome P450
DILI	Drug induced liver injury
DS	Discovery Studio
ESMs	Essential secondary metabolites
FDA	America food and drug admnistration
GIA	Gastrointestinal absorption
hACE2	human ACE2
hERG	Human ether-a-go-go-related gene
H-HT	Human hepatotoxicity
I	Inhibitor
Ki	Inhibition Constant
LD_{50}	Median lethal dose
Log K_p	Skin permeation
LogP	Lipophilicity
MD	Molecular docking
MERS-CoV	Middle East respiratory syndrome coronavirus
MR	Molecular refractivity
MW	Molecular weight
NCBI	National Center for Biotechnology Information
No Ar HA	Number of aromatic heavy atoms
No HA	Number of heavy atoms
No RB	Number of rotatable bonds
No.HBA	Number of hydrogen bond acceptors
No.HBD	Number of hydrogen bond donors
PDB	Protein data bank
P-gp	P-glycoprotein
RBD	Receptor-Binding Domain
RNA	Ribozome nucleic acid
S	Spike protein
SARS-CoV-2	Severe acute respiratory syndrome coronavirus-2
TMPRSS2	Transmembrane protease serine 2
TPSA	Topological polar surface area

SUPPLEMENTARY DATA

To be provided on request by the corresponding author.

REFERENCES

1. International Committee on Taxonomy of Viruses for Coronaviridae Study Group. The species severe acute respiratory syndrome- related coronavirus: classifying 2019-nCoV and naming it SARS- CoV-2. Nature Microbiology, 5, 2020: 536–544. doi: 10.1038/srep42717.
2. Zhou P, Yang XL, Wang XG, Hu B, Zhang L, Zhang W, Si HR, Zhu Y, Li B, Huang CL, Chen HD, Chen J, Luo Y, Guo H, Jiang RD, Liu MQ, Chen Y, Shen XR, Wang X, Zheng XS, Zhao K, Chen QJ, Deng F, Liu LL, Yan B, Zhan FX, Wang YY, Xiao GF, Shi ZL. A pneumonia outbreak associated with a new coronavirus of probable bat origin. Nature, 579(7798), 2020: 270–273. doi: 10.1038/s41586-020-2012-7.
3. Hoffmann M, Kleine-Weber H, Schroeder S, Krüger N, Herrler T, Erichsen S. "SARS-CoV-2 Cell Entry Depends on ACE2 and TMPRSS2 and Is Blocked by a Clinically Proven Protease Inhibitor". Cell, 181(2), 2020: 271-280. doi:10.1016/j.cell.2020.02.052.

4. Machhi J, Herskovitz J, Senan A, Dutta D, Nath B, Oleynikov M, Blomberg W, Meigs D, Hasan M, Patel M, Kline P, Chang R, Chang L, Gendelman H, Kevadiya B. The Natural History, Pathobiology, and Clinical Manifestations of SARS-CoV-2 Infections. Journal of Neuroimmune Pharmacology, 12, 2020: 123-132. doi: 10.1007/s11481-020-09944-5
5. Shang J, Wan Y, Luo C, Ye G, Geng Q, Auerbach A, Li F. Cell entry mechanisms of SARS- CoV-2. Proceedings of National Academy of Science of USA, 117, 2020: 11727–11734. doi: 10.1073/pnas.2003138117.
6. Walls AC, Park Y, Tortorici MA, Wall AT, McGuire AT, Veesler D. Structure, function, and antigenicity of the SARS- CoV-2 spike glycoprotein. Cell, 181, 2020: 281–292. doi: 10.1016/j.cell.2020.02.058.
7. Wan Y, Shang J, Graham R, Baric R S and Li F. Acceptor recognition by the novel coronavirus from Wuhan: an analysis based on decade- long structural studies of SARS coronavirus. Journal of Virology, 94, 2020: e00127-20.
8. Forster P, Forster L, Renfrew C, Forster M. Phylogenetic network analysis of SARS- CoV-2 genomes. Proceedings of National Academy of Science of USA, , 117, 2020: 9241–9243.
9. Prashanth GK, Krishnaiah GM. Chemical composition of the leaves of *Azadirachta Indica Linn (Neem)*. International Journal of Advancement in Engineering Technology, Management and Applied Science, 1(5), 2014: 21-31. doi: 10.4236/oalib.1104458.
10. Hossain MA, Nagooru MR. Biochemical profiling and total flavonoids contents of leaves crude extract of endemic medicinal plant, *Corydyline terminalis* L. Kunth. Pharmacognosy Journal, 3, 2011: 25-30. doi: 10.5530/pj.2011.24.5
11. Ghimeray AK, Jin CW, Ghimire BK, Che DH. Antioxidant activity and quantitative estimation of *Azadirachtin* and Nimbin in *Azadirachta indica*. African Journal of Biotechnology, 54, 2009: 1684–5315.
12. El-Hawary SS, El-Tantawy ME, Rabeh MA, Badr WK. Chemical composition and biological activities of essential oils of *Azadirachta indica* A. Juss. International Journal of Applied Research in Natural Products, 6, 2013: 33-42.
13. Pandey IP, Ahmed SF, Chhimwal S, Pandey S. Chemical composition and wound healing activity of volatile oil of leaves of *Azadirachta indica* A. juss. Advances in Pure and Applied Chemistry, 62, 2012: 2167-0854.
14. Biswas K, Chattopadhyay I, Banerjee RK, Bandyopadhyay U. Biological activities and medicinal properties of neem (*Azadirachta indica*). Current Science, 13, 2002:36-45.
15. Britto AJ, Sheeba DH. *Azadiracta indica* juss – a potential antimicrobial agent, International Journal of Applied Biological and Pharmaceutical Technology, 21, 2011: 4550–4557.
16. Muhammed D, Odey BO, Alozieuwa BU, Alawode RA, Okunlola BM, Ibrahim J, Lawal A, Berinyuy EB. Azadirachtin-A a bioactive compound from *Azadirachta indica* is a potential inhibitor of SARS-CoV-2 main protease. AROC in Pharmaceutical and Biotechnology, 1(1), 2021:1-8. doi: 10.53858/AROCPB01010108
17. Borkotoky S, Banerjee M. A computational prediction of SARS-CoV-2 structural protein inhibitors from *Azadirachta indica* (Neem). Journal of Biomolecular Structure and Dynamics, 8, 2020:1-11. doi: 10.1080/07391102.2020.1774419
18. Fernandes SR, Barreiros L, Oliveira RF, Cruz A, Prudêncio C, Oliveira AI, Pinho C, Santos N, Morgado J. Chemistry, bioactivities, extraction and analysis of azadirachtin: State-of-the-art. Fitoterapia, 134, 2019:141-150. doi: 10.1016/j.fitote.2019.02.006
19. Loganathan T, Barathinivas A, Soorya C, Balamurugan S, Nagajothi TG, Ramya S, Jayakumararaj R. GCMS Profile of Bioactive Secondary Metabolites with Therapeutic Potential in the Ethanolic Leaf Extracts of *Azadirachta indica*: A Sacred Traditional Medicinal Plant of INDIA. Journal of Drug Delivery and Therapeutics, 11(4-S), 2021 :119-126 doi: 10.22270/jddt.v11i4-S.4967.
20. Mohammad MS, Forough M. Investigation of Compounds from *Azadirachta indica* (Neem). Asian Journal of Plant Sciences, 6, 2007: 444-445. doi: 10.3923/ajps.2007.444.445
21. Kim S, Thiessen PA, Bolton EE, Chen J, Fu G, Gindulyte A, Han L, He J, He S, Shoemaker BA, Wang J, Yu B, Zhang J, Bryant SH. PubChem Substance and Compound databases. Nucleic Acids Res., 44(D1), 2016: D1202-13. doi: 10.1093/nar/gkv951..
22. Dong J, Wang N, Yao Z, Zhang L, Cheng Y, Ouyang D, Lu A, Cao D. ADMETlab: a platform for systematic ADMET evaluation based on a comprehensively collected ADMET database. Journal of Cheminformatics, 10, 2018: 29. doi: 10.1186/s13321- 018-0283-x
23. 23. Daina A, Olivier M, Vincent Z. SwissADME: a free web tool to evaluate pharmacokinetics, drug-likeness and medicinal chemistry friendliness of small molecules. Scientific Report, 7, 2017:42717.
24. Lipinski CA, Lombardo F, Dominy BW, Feeney PJ. Experimental and computational approaches to estimate solubility and permeability in drug discovery and development settings. Advanced Drug Delivery

Review, 46, 2001: 3-26. doi: 10.1016/s0169-409x(00)00129-0.

25. Burley SK, Bhikadiya C, Bi C, Bittrich S, Chen L, Crichlow GV, Christie CH, Dalenberg K, Di Costanzo L, Duarte JM, Dutta S, Feng Z, Ganesan S, Goodsell DS, Ghosh S, Green RK, Guranović V, Guzenko D, Hudson BP, Lawson CL, Liang Y, Lowe R, Namkoong H, Peisach E, Persikova I, Randle C, Rose A, Rose Y, Sali A, Segura J, Sekharan M, Shao C, Tao YP, Voigt M, Westbrook JD, Young JY, Zardecki C, Zhuravleva M. RCSB Protein Data Bank: powerful new tools for exploring 3D structures of biological macromolecules for basic and applied research and education in fundamental biology, biomedicine, biotechnology, bioengineering and energy sciences. Nucleic Acids Research, 49(**D1)**, 2021:D437-D451. doi: 10.1093/nar/gkaa1038.
26. Trott O, Olson AJ. AutoDock Vina: improving the speed and accuracy of docking with a new scoring function, efficient optimization and multithreading. Journal of Computational Chemistry; 31, 2010: 455-461.
27. Pettersen EF, Goddard TD, Huang CC, Couch GS, Greenblatt DM, Meng EC, Ferrin TE. UCSF chimera: a visualization system for exploratory research and analysis. Journal of Computational Chemistry, 25, 2004: 1605-1612. doi: 10.1002/jcc.20084.
28. Biovia DS. Discovery Studio Visualizer v21.1.0.20298. San Diego. 2021. https://discover.3ds.com/discovery-studio-visualizer
29. Pajouhesh H, Lenz GR. "Medicinal Chemical Properties of Successful Central Nervous System Drugs". *Journal of American Society for Experimental Neuro Therapeutics*, 2(4), 2005: 541-553. doi*:*10.1602/neurorx.2.4.541.
30. Mannhold R, Poda GI, Ostermann C. Calculation of molecular lipophilicity: State-of-the-art and comparison of logP methods on more than 96,000 compounds. Journal of Pharmaceutical Science, 98, 2009: 861–893.
31 Cheng T, Zhao Y, Li X, Lin F, Xu Y, Zhang X, Li Y, Wang R, Lai L. Computation of Octanol−Water Partition Coefficients by Guiding an Additive Model with Knowledge. Journal of Pharmaceutical Science, 47(6), 2007: 2140–2148. doi: 10.1021/ci700257y.
32 Wildman SA, Crippen GM. Prediction of Physicochemical Parameters by Atomic Contributions. Journal of Chemical Information and Computer Sciencee, 39, 1999: 868–873.
33 Moriguchi I, Shuichi H, Nakagome I, Hirano H. Comparison of reliability of logP values for Drugs calculated by several methods. Chemical and Pharmaceutical Bulletin, 42, 1994: 976–978.
34 Martin S, Roe D, Faulon JL. Predicting protein-protein interactions using signature products. Bioinformatics, 21(2), 2005: 218-226. doi: 10.1093/bioinformatics/bth483
35 Potts RO, Guy RH. Predicting skin permeability. Pharmaceutical Research, 9(5), 1992: 663-669. doi: 10.1023/a:1015810312465.
36 Szakács G, Váradi A, Ozvegy-Laczka C, Sarkadi B. The role of ABC transporters in drug absorption, distribution, metabolism, excretion and toxicity (ADME-Tox). Drug Discovery Today, 13, 2008: 379–393. doi: 10.1002/cbdv.200900022.
37 Lei T, Li Y, Song Y, Li D, Sun H, Hou T. ADMET evaluation in drug discovery: Accurate prediction of rat oral acute toxicity using relevance vector machine and consensus modeling. Journal of Cheminformatics, 8(6), 2016: 1-19.
38 Cournia Z, Allen B, Sherman W. Relative binding free energy calculations in drug discovery: recent advances and practical considerations. J Chem Inf Model, 57, 2017: 2911-2937. doi: 10.1021/acs.jcim.7b00564.